

Fourier transform infrared spectroscopic imaging of cardiac tissue to detect collagen deposition after myocardial infarction

Rabee Cheheltani
Jenna M. Rosano
Bin Wang
Abdel Karim Sabri
Nancy Pleshko
Mohammad F. Kiani

Fourier transform infrared spectroscopic imaging of cardiac tissue to detect collagen deposition after myocardial infarction

Rabee Cheheltani,^a Jenna M. Rosano,^a Bin Wang,^{a,b} Abdel Karim Sabri,^c Nancy Pleshko,^d and Mohammad F. Kiani^{a,e}

^aTemple University, Department of Mechanical Engineering, Philadelphia, Pennsylvania

^bWidener University, Department of Biomedical Engineering, Chester, Pennsylvania

^cTemple University School of Medicine, Department of Physiology, Cardiovascular Research Center, Philadelphia, Pennsylvania

^dTemple University, Department of Bioengineering, Philadelphia, Pennsylvania

^eTemple University School of Medicine, Department of Radiation Oncology, Philadelphia, Pennsylvania

Abstract. Myocardial infarction often leads to an increase in deposition of fibrillar collagen. Detection and characterization of this cardiac fibrosis is of great interest to investigators and clinicians. Motivated by the significant limitations of conventional staining techniques to visualize collagen deposition in cardiac tissue sections, we have developed a Fourier transform infrared imaging spectroscopy (FT-IRIS) methodology for collagen assessment. The infrared absorbance band centered at 1338 cm^{-1} , which arises from collagen amino acid side chain vibrations, was used to map collagen deposition across heart tissue sections of a rat model of myocardial infarction, and was compared to conventional staining techniques. Comparison of the size of the collagen scar in heart tissue sections as measured with this methodology and that of trichrome staining showed a strong correlation ($R = 0.93$). A Pearson correlation model between local intensity values in FT-IRIS and immuno-histochemical staining of collagen type I also showed a strong correlation ($R = 0.86$). We demonstrate that FT-IRIS methodology can be utilized to visualize cardiac collagen deposition. In addition, given that vibrational spectroscopic data on proteins reflect molecular features, it also has the potential to provide additional information about the molecular structure of cardiac extracellular matrix proteins and their alterations. © 2012 Society of Photo-Optical Instrumentation Engineers (SPIE). [DOI: [10.1117/1.JBO.17.5.056014](https://doi.org/10.1117/1.JBO.17.5.056014)]

Keywords: Fourier transform infrared spectroscopy; cardiac remodeling; collagen; myocardial infarction; cardiac extracellular matrix.

Paper 11745 received Dec. 13, 2011; revised manuscript received Mar. 2, 2012; accepted for publication Mar. 5, 2012; published online May 11, 2012.

1 Introduction

Extracellular matrix (ECM) is a key component and regulator of many biological tissues. In cardiac tissue, this matrix supports, connects, and coordinates cardiac myocytes and the forces generated by them.^{1,2} Several cardiac pathologies are associated with significant changes in the composition of the matrix.^{1,2} Therefore, detection and quantitative measurement of these matrix changes play an important role in experimental assessment of novel treatment methods and drug delivery systems for treating cardiac diseases. Adverse cardiac remodeling and cardiac fibrosis after myocardial infarction is one of the most commonly studied aspects of ECM alteration in cardiac tissue. This fibrosis may be characterized by replacement of dead cardiomyocytes with fibrillar collagen and formation of scar tissue in the infarct zone as well as excessive deposition of fibrous tissue in interstitium remote to infarction site.^{1,3} This change in tissue composition leads to increased stiffness and eventually cardiac dysfunction.^{3,4} Several assays have been developed to assess the excess collagen deposition in cardiac tissue. Histochemical assays such as trichrome or picrosirius red staining protocols are some of the most common methods of visualizing collagen deposition in heart sections.^{3,5} Immunohistochemical

staining methods provide a more specific, sensitive, and quantifiable staining technique but they use expensive reagents and achieving reliable results require substantial preparation and experimentation.^{6,7} In this study, Fourier transform infrared imaging spectroscopy (FT-IRIS) is proposed as an alternative or complementary method to these conventional assays.

In Fourier transform infrared (FTIR) spectroscopy, the interaction of molecular bonds with varying wavelengths of infrared light are measured. Molecular structures inside the matter under study (such as biological tissues) can be characterized based on signature spectral absorbances.⁸ The coupling of an FTIR spectrometer to a microscope and array detector provides an imaging system for creation of maps of molecular bond vibrations, known as hyperspectral imaging, or Fourier transform infrared imaging spectroscopy, FT-IRIS.⁹ Data collection in FT-IRIS does not require staining or labeling prior to imaging, and thus is not prone to batch to batch variability. Furthermore, unlike histochemical techniques, this technology has the potential for *in vivo* use through fiber optic applications.^{10,11} FTIR and FT-IRIS have been applied to analyze several soft¹² and hard¹³ tissue types including bone and cartilage,⁹ skin,¹⁴ and arteries¹⁵; however, the study of their applicability to cardiac tissue has been limited so far.

Liu et al. identified a number of IR absorption peaks that are characteristic of collagen using single point mid-infrared spectra of infarcted rat left ventricle compared with sham control,¹⁶ but no

Address all correspondence to: Mohammad F. Kiani, Temple University, Department of Mechanical Engineering, 1947 North 12th Street, Philadelphia, Pennsylvania. Tel.: (215) 204-4644; Fax: (215) 204-4956; E-mail: mkiani@temple.edu

quantitative analysis was performed. In a later study¹⁷ the authors used an absorbance band at 1204 cm^{-1} as the representative band for collagen deposition. They used the intensity of the inverted second derivative of the 1204 cm^{-1} band to qualitatively show similar collagen localization between the spectroscopic analysis and trichrome staining of the tissue. However, the 1204 cm^{-1} band is part of the amide III absorbance that is present in some form in all proteins, including the major component of cardiac tissue, myosin, and therefore is not necessarily a very specific spectroscopic marker. In another study,¹⁸ attenuated total reflectance (ATR) spectroscopy was used to classify normal and cardiomyopathic hamster heart tissue through linear discrimination analysis aided by genetic algorithm selection of spectroscopically diagnostic mid-IR regions. In that study, specific absorbances attributable to cardiac collagen were not identified. In a later study by the same author,¹⁹ synchrotron FTIR was utilized to assess cardiomyopathic hamster heart for collagen expression in focal microdomains based on similarities in the tissue spectra and that of pure collagen in the amide III range (1167 to 1355 cm^{-1}). Here again, no specific collagen absorbances were identified in the cardiac tissue spectra. Finally, a recent FTIR imaging study by Yang et al.²⁰ evaluated collagen deposition in a human heart post-MI based on the 1638 cm^{-1} absorbance found in the amide I region. In this study, qualitative comparisons were made to H&E staining, but no comparisons to histologic staining specific for collagen were performed. Overall, these prior studies that utilized FTIR to qualitatively assess collagen demonstrate the potential for quantitative characterization of collagen deposition in cardiac tissue using FTIR technology.

The objective of the current study was to (a) introduce standard FT-IRIS methodology for creating distribution maps of collagen in remodeled cardiac tissue sections and (b) quantitatively compare maps created by FT-IRIS with conventional staining techniques. This distribution mapping can be utilized to visualize collagen deposition when assessing the results of treatment strategies involving ECM. Therefore, this methodology was also applied to map collagen deposition in infarcted rat cardiac tissues that showed moderated cardiac remodeling after treatment with targeted delivery of vascular endothelial growth factor (VEGF).^{21,22}

2 Materials and Methods

2.1 Induction of MI

All animal procedures were performed under an IACUC-approved protocol. Myocardial infarction was surgically induced in six-week-old male Sprague-Dawley rats (Harlan Laboratories, Indianapolis, IN) as described previously.²³ Briefly, rats were anesthetized with 4% isoflurane and maintained with 2% isoflurane using a rodent respirator. After a left thoracotomy, and pericardiotomy, the heart was exteriorized and a 6.0 silk suture was placed around the left anterior descending coronary artery and ligated. The heart was placed back and the chest was closed. The lungs were then reinflated using positive end-expiratory pressure. Animals were then allowed to recover.

2.2 Targeted Delivery of VEGF Treatment

To demonstrate the applicability of our methodology to drug delivery and treatment development, a group of infarcted rats were treated by targeted delivery of VEGF to infarcted myocardium and the extent of collagen deposition in their

cardiac tissue was compared to control group ($n = 6$ in each group). For treatment group, upon completion of the surgical procedure, animals received targeted delivery of VEGF-encapsulated immunoliposomes via tail vein injection. We have previously shown that this treatment improves cardiac function and vascular structure in MI rats.²¹

2.3 Extraction of Heart Samples and Cryopreservation

Four weeks after the induction of MI, rats were anesthetized with ketamine/xylazine $87/13\text{ mg/kg}$ S.C. and euthanized by cardiectomy. Excised hearts were washed in saline solution, placed in embedding medium (Tissue-Tek O.C.T Compound, Sakura Finetek, Torrance, CA), and flash frozen in a mixture of dry ice and isopentane. Fresh frozen tissues were kept at -80°C until sectioning.

2.4 Cryo-Sectioning

For FT-IRIS analysis, $9\text{-}\mu\text{m}$ sections of unfixed frozen tissue embedded in embedding medium were mounted on low-e reflective-coated infrared microscope slides (MIRIR slides, Kevley Technologies, Chesterland, OH). Sections were then air-dried for 30 min, embedding medium dissolved in deionized water, and sections fixed in 10% formalin and air dried completely. For immunohistochemical and histologic analysis, $9\text{ }\mu\text{m}$ sections of unfixed frozen tissue were mounted on polylysine coated slides. All sections used in immunohistochemical staining were collected consecutively after the corresponding section used for FT-IRIS analysis. For some histochemical staining samples, sections were not consecutive to their paired sections obtained for FT-IRIS.

2.5 FT-IRIS Data Acquisition and Analysis

FT-IRIS images of a section of the heart on low-e slides were acquired at $25\text{ }\mu\text{m}$ (partial tissue sections) or $50\text{ }\mu\text{m}$ (whole tissue sections) pixel resolution and 8 cm^{-1} spectral resolution with two co-added scans using a Perkin Elmer Spotlight 400 spectrometer (Shelton, CT). The spectrometer source is an electrically heated silicon carbide light source with high emissivity and a quasi-blackbody emission spectrum with an effective temperature of $\sim 1300\text{ K}$. Data were analyzed with Isys 5.0 software (Spectral Dimensions Inc., Olney, MD). The integrated area of the amide I absorbance band, centered near 1650 cm^{-1} , that arises from the $\text{C}=\text{O}$ stretching vibration,⁹ was used to mask each sample such that only tissue regions of the image were included in analyses. The baselined, integrated area of the absorbance band centered at 1338 cm^{-1} , arising from collagen CH_2 side chain vibrations,¹¹ was mapped across the tissue section, creating an intensity image of collagen deposition [Fig. 1(a)–1(e)]. As the 1338 cm^{-1} is a very small absorbance band, we also performed second derivative analysis on the spectra to confirm the distribution at that wavenumber [Fig. 1(f) and 1(g)]. Second derivative spectra can be utilized to improve the resolution of absorbance bands, while maintaining a relationship to intensity of the original raw spectral absorbance band.²⁴ The results of these analyses were similar to the integrated absorbance band analysis, and thus only the integrated band areas are presented in the Results section.

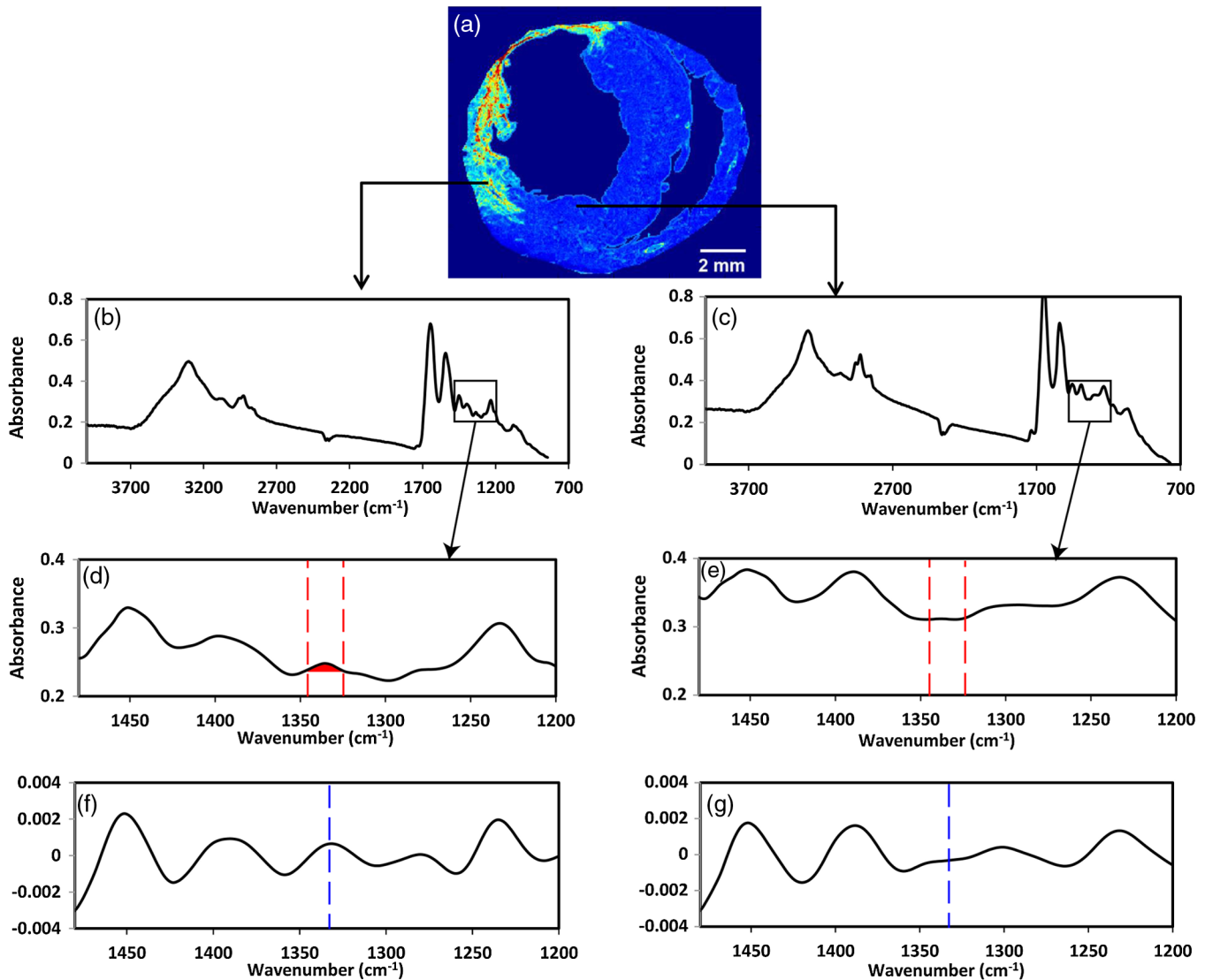


Fig. 1 FTIR spectra of myocardial tissue. (a) Intensity image created by peak integration mapping of the 1338 cm^{-1} absorbance band that arises from collagen sidechain vibrations. (b) Representative spectra for left ventricle within the infarct region. (c) Representative spectra for left ventricle remote to the infarct region. Expanded spectra in (d) the infarcted myocardium and (e) myocardium remote to the infarct region showing the area of integration for 1338 cm^{-1} absorbance in (d), and the absence of the absorbance in (e). Expanded inverted second derivative spectra (multiplied by negative one to facilitate peak identification) in (f) the infarcted myocardium and (g) myocardium remote to the infarct region.

2.6 Immunohistochemical Staining for Collagen Type I

Immunohistochemical staining was used to visualize the distribution of collagen type I in the infarct zone of rat heart sections. Since cardiac collagen type I is the primary collagen type in cardiac fibrosis,^{2,25} collagen type I was selected as the target molecule for the staining. Briefly, $9\text{-}\mu\text{m}$ cross-sections of fresh frozen heart tissue on polylysine coated slides were incubated with 5% BSA in PBS to block unspecific binding, and then incubated at 4°C overnight with mouse monoclonal to Collagen I antibody (abcam Ab90395, 1:200 dilution) diluted in 5% BSA in PBS. Slides were then washed in PBS, incubated with Alexa Fluor 594 donkey anti-mouse IgG (Invitrogen A21203, 1:200 dilution in PBS), washed in PBS, incubated with DAPI, washed in PBS, and mounted with glass coverslips using mounting medium for fluorescence (Vectashield, Vector Laboratories, Burlingon, CA). Images of the stained slides

were taken using a Retiga 1300 microscope camera (QImaging, Surrey, BC) and Mac 5000 motorized stage controller (Ludl Electronics, Hawthorne, NY) coupled to a Nikon Eclipse TE200 (Nikon Instruments Inc., Melville, NY) fluorescent microscope.

2.7 Histological Staining

Gomori's trichrome stain (Richard Allen Scientific, Kalamazoo, MI) was used to histochemically distinguish collagen (blue) from muscle tissue (red). Nine-micrometer cross-sections of fresh frozen heart tissue mounted on histology slides were fixed with Bouin's solution at 56°C for 1 h, and then stained according to the manufacturer's directions. Stained heart sections were dehydrated using various grades of alcohol and xylenes, and then mounted with glass cover-slips. Images of sequential regions within each section were obtained using a Nikon DS-Fi1 color microscope camera and Nikon Element

software (Nikon Instruments, Inc., Melville, NY). A mosaic image of the area of interest was created using Adobe Photoshop CS software.

Picosirius red (Polysciences, Inc.) stains thick collagen fibers bright yellow to red when viewed under polarized light²⁶ and was also used to show collagen deposition in the infarct zone. Nine-micrometer sections of fresh frozen heart tissue were obtained on polylysine coated slides. Heart sections were fixed with 4% formaldehyde for 10 min, and then stained according to the manufacturer's directions, dehydrated and mounted with glass slides. Images of sequential regions within each section were obtained under polarized light using a Nikon Digital DS-Fi1 color camera and Nikon Element software. A mosaic image of the area of interest was created using Adobe Photoshop CS software.

2.8 Image Processing

Six infarcted heart tissue samples were used to compare FT-IRIS local intensity of collagen deposition with immunohistochemical staining. Collagen intensity maps were created on two consecutive 9- μm sections of infarcted myocardium using FT-IRIS and fluorescent microscopic imaging of immunohistochemical staining as described above. Images from both techniques were imported into ImageJ software as 8-bit grayscale intensity images, resized and aligned to match. The same area of $6250 \times 1875 \mu\text{m}$ containing the scar region was selected in both images, and after normalizing the intensity by adjusting the minimum to 0 and maximum to 255 in both, each were divided into a 5×4 grid (Fig. 2, panel a). The mean gray value in each element of the grid was measured and the gray values from two methods were compared for 20 grid elements in a Pearson's correlation analysis (Fig. 2, panel b).

Nine samples (four targeted VEGF-treated and five untreated control MI animals) were used to compare area of collagen deposition in cardiac sections from FT-IRIS images with trichrome staining results by correlating the number of pixels denoting collagen deposition in each section from both methods. In FT-IRIS intensity images, the 1338 cm^{-1} peak integration values above zero were used as a threshold to create a binary image of the cross section, isolating areas of collagen deposition from the rest of the tissue. These images were processed in ImageJ software (the National Institutes of Health, USA) to measure the percentage area of the scar region in each tissue cross section. In trichrome images, scar region was isolated using ImageJ software. First a color deconvolution routine²⁶ was performed (using the ImageJ plug-in) to separate RGB channels. In the blue channel, a threshold was applied at a level that distinguished stained areas (denoting scar region) from the unstained background followed by noise reduction procedures. The percentage area of stained regions (collagen deposition) within each sample was measured.

2.9 Statistical Data Analysis

Data analysis was performed with statistical software Sigmaplot (Systac Software Inc., San Jose, CA). Correlation coefficients (R values) were calculated from a Pearson's correlation model with P values less than 0.05 considered to be statistically significant. Comparison of treatment groups was performed using a student's T-test.

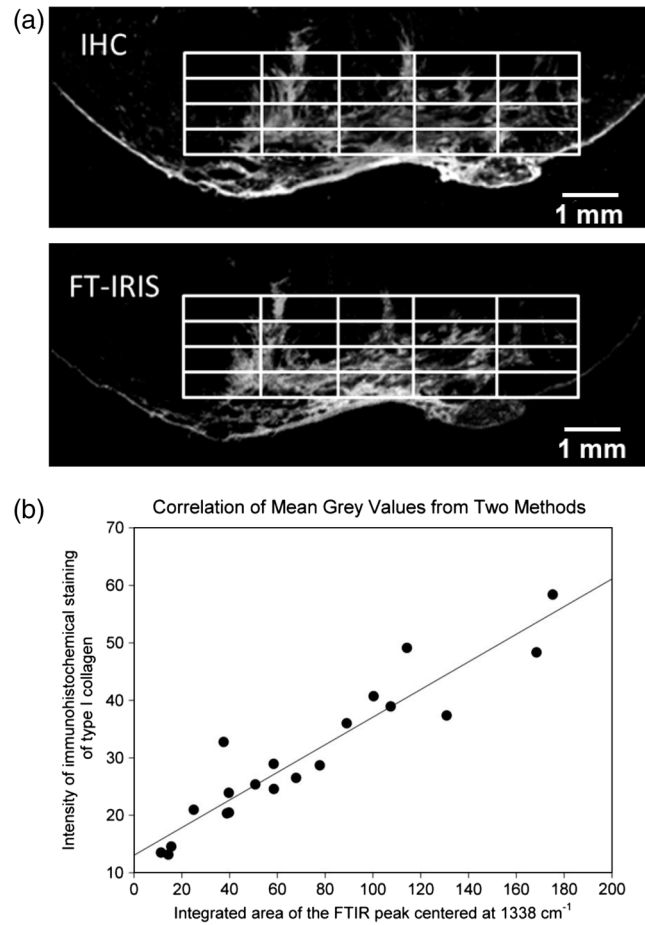


Fig. 2 Comparison of intensity maps from FT-IRIS and immunohistochemical staining (IHC) in a representative sample. Panel a shows the image of the infarct region from both techniques after being resized and aligned to match. A grid of 5×4 was applied to the same area of $6250 \times 1875 \mu\text{m}$ in both images. In panel b, mean gray values in each grid element were compared between two methods in a Pearson correlation model.

3 Results

3.1 Qualitative Correlation of FT-IRIS Data Versus Staining Methods

Peak integration mapping of the band centered at 1338 cm^{-1} creates a map of collagen deposition consistent with images created by three different staining techniques in serial sections of the infarct zone in the same rat heart sample (Fig. 3). Panel a shows an FT-IRIS obtained color map of the collagen deposition density with red being the highest and blue the lowest. Immunohistochemical staining of collagen type I of the same tissue (panel b) demonstrates the same density distribution as the FT-IRIS image. In Gmori's trichrome staining of an adjacent section from the same tissue (panel c) collagen deposition stained in blue, distinguished from red stained muscle tissue, appears in the same areas as in the FT-IRIS image. For panel d, a section from the same tissue was stained using a picosirius red staining protocol as described above and imaged under polarized light. The bright red and yellow collagen fibers again show a similar distribution as other staining techniques and FT-IRIS image. We also compared FT-IRIS mapping based on the inverted second derivative peak at 1204 cm^{-1} ,¹⁷ but did not find any collagen-specific results (data not shown).

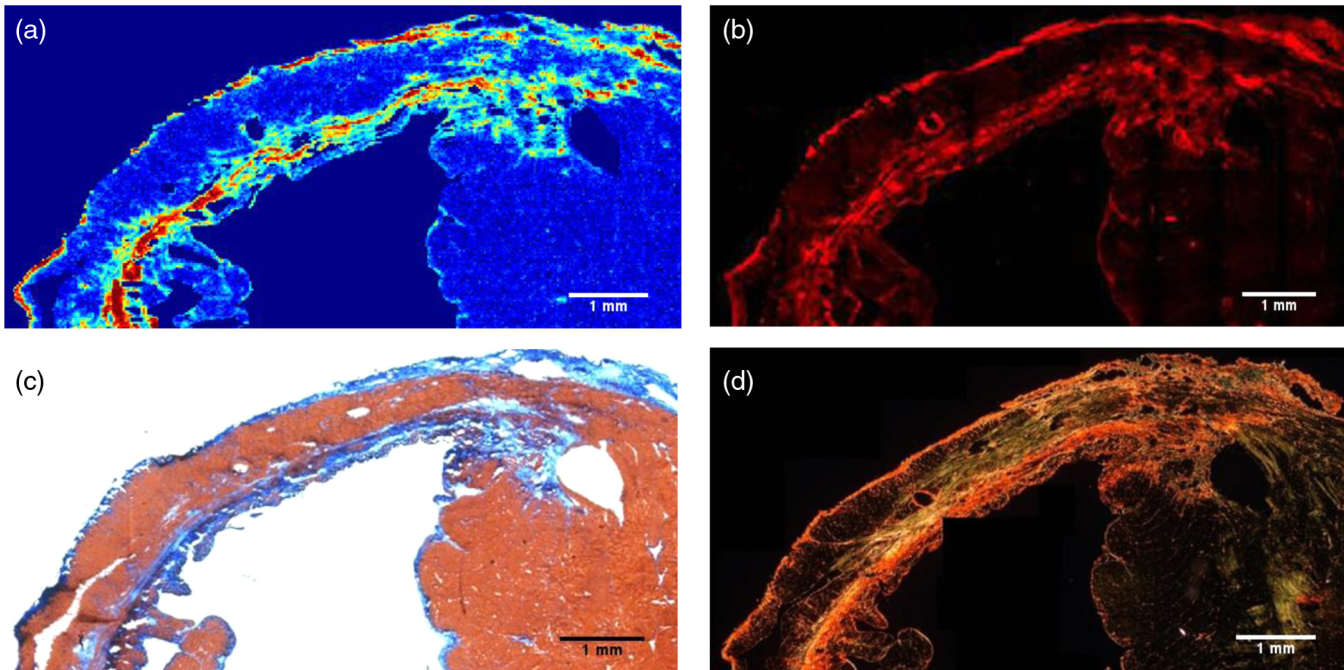


Fig. 3 Collagen deposition is mapped in infarcted left ventricle using FT-IRIS imaging of the 1338 cm^{-1} absorbance (a), immunohistochemical staining of collagen type I (b), trichrome staining (c), and picosirius red staining under polarized light (d).

3.2 FT-IRIS to Map Collagen Deposition Density

Figure 4 shows correlation of local mean gray values, representing collagen deposition density, between immunohistochemical staining of type I collagen and FT-IRIS map of collagen deposition in a consecutive section for six different MI control samples. As demonstrated in these graphs and their corresponding correlation coefficient values, FT-IRIS maps of the collagen deposition density strongly correlates with immunohistochemical staining results (average correlation coefficient of six samples = 0.86 ± 0.07 , $p < 0.01$ for all samples). A similar strong correlation between the two methods was observed in samples treated with targeted delivery of VEGF to infarcted myocardium (data not shown).

3.3 FT-IRIS to Measure Extent of Collagen Deposition

Using the methods described, infarct collagen scar areas in FT-IRIS images of heart sections were isolated from the rest of the tissue by creation of a binary image, and were compared to images from the same tissue samples stained with Gmori's trichrome protocol. The results from the two methods strongly correlated (Fig. 5) in a Pearson's correlation model with correlation coefficient value of 0.93, $p < 0.01$. In addition, animals treated with targeted delivery of VEGF to infarcted myocardium show a reduced size of collagen scar compared to untreated animals as assessed by FT-IRIS ($1.6 \pm 6.9\%$ versus $18.7 \pm 3.9\%$, respectively, $P = 0.052$). These results are consistent with earlier studies that showed targeted delivery of VEGF to MI tissue reduces collagen deposition in the MI area.^{21,22}

4 Discussion

Cardiac remodeling involves cellular and structural processes affecting myocytes and their contractile proteins as well as extracellular matrix.²⁷ This matrix, primarily composed of collagen,^{1,2} undergoes a remodeling process in most cardiac disease

conditions resulting in an increase in collagen deposition and fibrosis.¹ The extent of fibrosis and collagen scar is an important factor in the assessment of interventions aimed at treating cardiac diseases.² Hence an efficient and reliable measurement of collagen deposition in cardiac tissue is of great interest in the assessment of treatment strategies for cardiac pathologies. Because of several limitations and the variability experienced in staining techniques, we propose an alternative FT-IRIS methodology for detection and characterization of collagen deposition in cardiac tissue.

The FTIR absorbance band centered at 1338 cm^{-1} arises from the amino acid side chain vibrations in collagen and was first identified by Jackson et al.²⁸ They attributed this band to CH wagging vibration of proline side chains. Infrared spectra from different collagen types in previous studies also show the existence of this band in, e.g., collagen type I and III,²⁹ type II¹¹ and type I and IV.³⁰ The intensity of this absorbance has been utilized to quantify triple helix collagen fibers in collagenase-induced cartilage degradation,³¹ as well as in osteoarthritic tissues.^{11,32} In the current study, the quantification of the local 1338 cm^{-1} band intensity across the section was utilized to map the extent of collagen deposition after myocardial infarction in rat heart tissue sections, and the results were comparable to conventional histology and immunohistochemical staining techniques. Other infrared absorbance bands, including the amide I carbonyl stretching mode of proteins, were investigated to assess collagen distribution, but only the 1338 cm^{-1} absorbance was found to be specific for collagen. As amide absorbance bands are found in all proteins, it is likely that the presence of the cardiac protein myosin, which also contains absorbances in these regions, precludes specificity of those bands for collagen in cardiac tissue.

Trichrome staining techniques are widely used for differentiation of collagen from muscle tissue and assessment of collagen deposition.³³ Although several hypotheses have been proposed to explain the differential tissue coloring of these

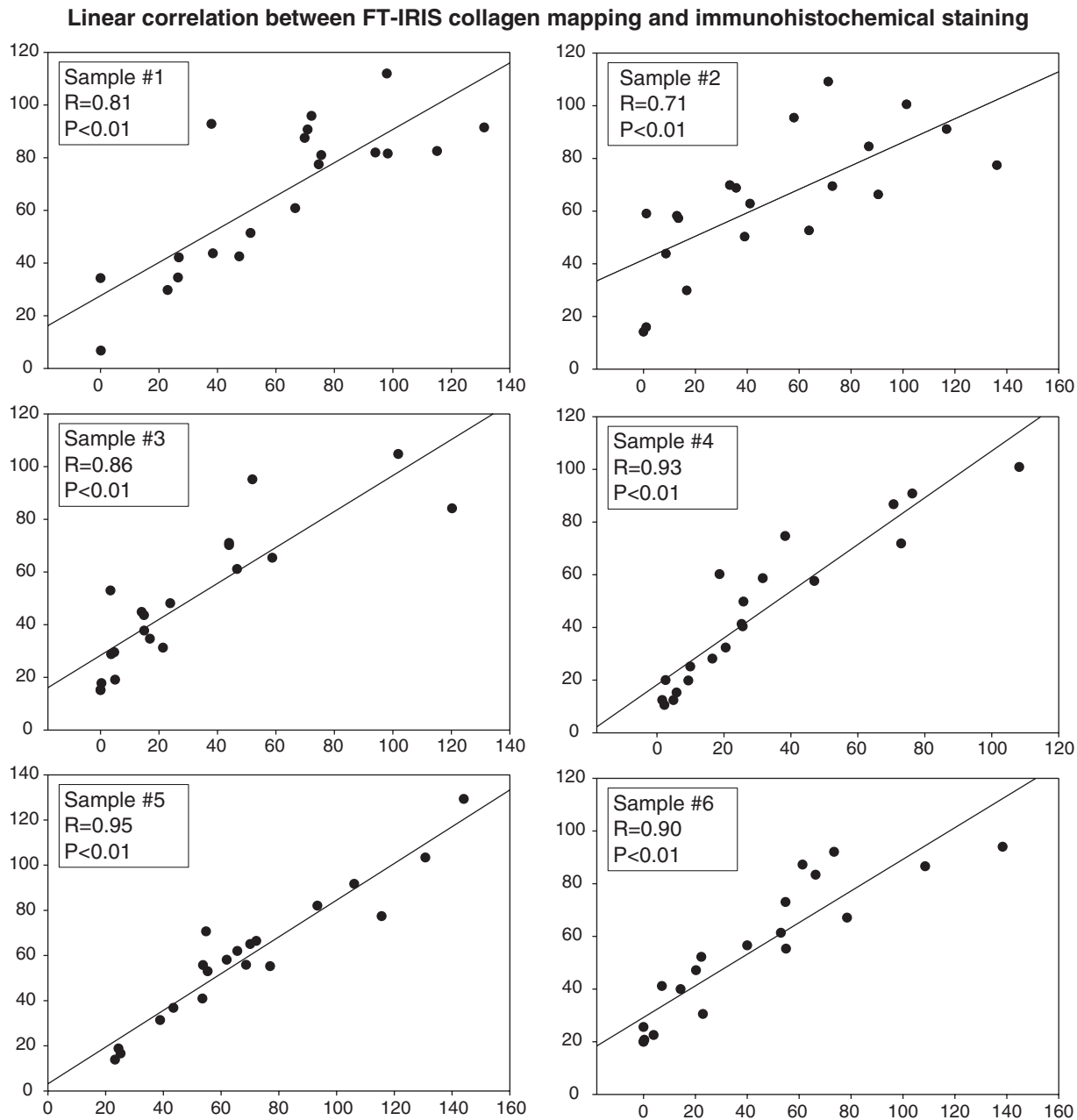


Fig. 4 Pearson correlation for local collagen intensity between the FT-IRIS method and immunohistochemical staining in consecutive sections from six samples. In each sample, mean gray values of 20 sequential grid elements were measured and correlated in intensity images created from integrated area of the band centered at 1338 cm^{-1} (X axis) versus immunohistochemical staining of collagen type I (Y axis) (average R for six samples = 0.86 ± 0.07 , average p value for six samples = 0.00007).

techniques, which use anionic dyes in association with heteropolycarboxylic acids, the exact mechanism is not completely understood.³⁴ Previous studies have used these methods to visualize collagen deposition and measure the size of the scar in diseased cardiac tissues.^{3,3,35} We have shown that the scar size measured as percentage of tissue section showing collagen deposition from FT-IRIS analysis strongly correlated with the measurements achieved by trichrome staining of a section from same heart tissues. The fact that samples used in this analysis were comprised of two groups of animals, a treatment group with

targeted delivery of VEGF to infarcted myocardium and a control untreated group, demonstrates the applicability of the methodology for different treatment conditions. We also used this methodology to show that a group of animals treated with targeted delivery of VEGF to infarcted myocardium, demonstrate a smaller collagen scar compared to controls, as was previously shown using conventional staining techniques. This provides an example of how this methodology could be used in the assessment of the size of the collagen scar in cardiac tissues independent of other staining techniques.

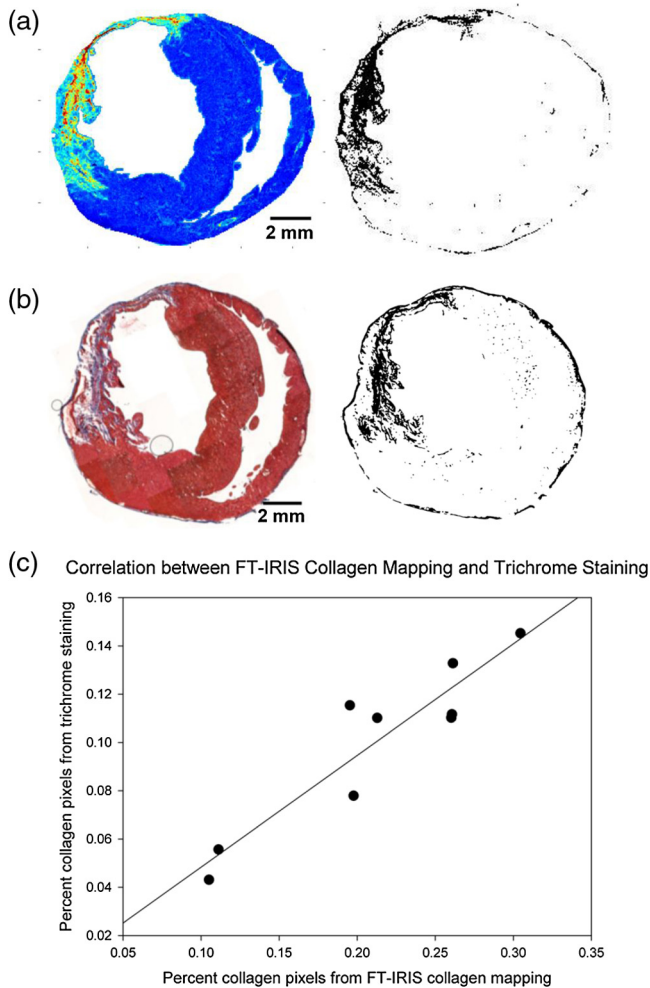


Fig. 5 Comparison of FT-IRIS and trichrome staining. (a) FT-IRIS mapping of collagen deposition in a typical sample (1338 cm^{-1} area) and the corresponding binary image separating collagen from the rest of the myocardium. (b) Trichrome staining of the sample tissue with the corresponding binary image. (c) Percentage area of collagen deposition in tissue sections (number of pixels) from the two methods in a Pearson correlation model. ($R = 0.93$, $P = 0.0003$).

Picrosirius red is another widely used staining method that interacts with collagen by the reaction of its sulphuric acid groups with the basic groups of collagen.³⁶ Picrosirius red stains fibrillar collagen more specifically and more precisely than trichrome staining techniques,^{3,5} especially when viewed under circularly polarized light since it no longer depends on the observation of a specific color but rather the birefringence of fibrillar collagen, which is a fundamental physical property.⁵ Although the dependence of brightness to collagen fiber orientation with respect to transmission axis of linear polarizer can be mitigated by use of circularly polarized light, attempts to quantify collagen volume fraction from the level of birefringence brightness are limited by the dependence of brightness to collagen fiber orientation relative to the section plane.⁵ Another complication with this technique is the necessity to exclude other noncollagen birefringent components of the tissue such as fibrin.³⁷

Immunohistochemical staining has been used to semiquantitatively assess the amount of different collagen types in cardiac fibrosis and remodeling.^{38–40} In our study, FT-IRIS and immu-

nohistochemical staining of type I collagen were strongly correlated in a linear model, thus verifying that the intensity of the 1338 cm^{-1} band can be utilized to evaluate collagen deposition density. This finding is consistent with the fact that in both methods the intensity is linearly correlated to the target molecule concentration, following the Beer-Lambert law.^{8,41} Scattering of infrared radiation could also occur as a result of tissue thickness, which would result in intensity changes. However, as our spectral absorbance values were on the order of 1 absorbance unit or less, it is unlikely that this is a major concern in the current study. The small variation observed between the two methods may be due to different methodologies for tissue preparation and measurement, as well as the fact that staining and FT-IRIS data were obtained from successive sections of the same tissue. In addition, the phenomena that give rise to the image intensities are different; in the case of FT-IRIS, image intensity is a measure of molecular vibrations, whereas in immunofluorescence, the level of chromophore binding is being imaged. In our imaging system, we confirmed that the fluorescence intensity of the primary-secondary antibody complex is linearly correlated to the concentration of the primary antibody (data not shown).

Creation of collagen distribution maps using FT-IRIS technology has several advantages over commonly utilized staining techniques. The spectra are acquired in a single microscopic scanning step after sectioning, thus it requires minimal tissue preparation and no additional reagents or hazardous histology chemicals. Furthermore, after an initial identification and analysis of the corresponding band (or bands, in multivariate analysis) to molecules of interest, the procedure could be repeated with additional tissue samples without variability among batches. In addition, since no target-specific staining is required, several different tissue components (e.g., different proteins, lipids, proteoglycans, etc.) can be studied on the same sample section as long as the corresponding absorbance bands are known. FTIR spectra can be acquired at pixel resolutions higher than $25\text{ }\mu\text{m}$ used in this study, and can be further enhanced in conjunction with an ATR accessory.⁴² For this study, however, changes in the pixel resolution from 6.25 to $50\text{ }\mu\text{m}$ did not affect the results (data not shown), since collagen density was mapped in relatively large areas of cardiac tissue.

The percentage change in collagen deposition after myocardial infarction depends on the severity of infarction and the extent of the remodeling process. In the tissue samples evaluated in the current study, the infarct scar comprised an average of 21% of the tissue cross section. The correlations between the FT-IRIS results and staining techniques confirms that the FT-IRIS method developed is indeed sensitive to collagen deposition in the range that is normally observed within the infarct scar. The infarct scar, however, is predominantly composed of collagen.⁴ If this technique is to be applied for the detection of very small percentages of collagen to other tissue components, a careful assessment of the sensitivity of the technique may be required. Previous studies have confirmed the sensitivity of FTIR in detection of very low (nM) concentrations of proteins using ATR methods,^{43–45} and concentrations on the order of $\sim 1\%$ in transmittance studies.^{46,47}

The motivation for further investigation of FTIR spectra and their band signatures in cardiac tissue is twofold. First, the capability of FTIR spectra in characterizing cardiac tissue is not limited to mapping collagen density. Although single absorbance band analysis was the focus of the present study, there

is a plethora of data in FTIR spectra, which if further investigated could yield valuable information about different cardiac proteins. Such information could answer some of the classical questions in cardiac remodeling and fibrosis such as differentiation and quantification of the ratio of different collagen types, or the extent and timeline of collagen cross-linking and maturity. The current FT-IRIS results do not distinguish between types I and III collagen, but it is possible that further investigations could result in this differentiation. The second potential lies in translation of this technology to *in vivo* diagnostic strategies. For example, this methodology can be used in the emerging area of catheter-based infrared fiber optics⁴⁸ to assist in the *in vivo* assessment of the health of cardiovascular tissues. In summary, the results presented support the further use, and clinical translation, of infrared spectral techniques for evaluation of cardiac pathologies and therapeutics.

Acknowledgments

Rabee Cheheltani is a predoctoral fellow of the American Heart Association. This work was supported by grants from the American Heart Association, and the National Institutes of Health.

References

1. K. T. Weber, "Cardiac interstitium in health and disease: the fibrillar collagen network," *J. Am. Coll. Cardiol.* **13**(7), 1637–1652 (1989).
2. S. de Jong et al., "Biomarkers of myocardial fibrosis," *J. Cardiovasc. Pharmacol.* **57**(5), 522–535 (2011).
3. Y. Sun and K. T. Weber, "Animal models of cardiac fibrosis," *Methods Mol. Med.* **117**(III), 273–290 (2005).
4. Y. Sun et al., "Infarct scar as living tissue," *Basic Res. Cardiol.* **97**(5), 343–347 (2002).
5. P. Whittaker et al., "Quantitative assessment of myocardial collagen with picrosirius red staining and circularly polarized light," *Basic Res. Cardiol.* **89**(5), 397–410 (1994).
6. R. T. Miller, "Technical immunohistochemistry: achieving reliability and reproducibility of immunostains," *Soc. Appl. Immunohistochem.* (2001) p. 56. http://www.ihcworld.com/_books/Miller_handout.pdf
7. J.-M. Fritschy, "Is my antibody-staining specific? How to deal with pitfalls of immunohistochemistry," *Eur. J. Neurosci.* **28**(12), 2365–2370 (2008).
8. B. C. Smith, *Fundamentals of Fourier Transform Infrared Spectroscopy*, CRC Press, Boca Raton, FL (1996).
9. A. Boskey and N. Pleshko Camacho, "FT-IR imaging of native and tissue-engineered bone and cartilage," *Biomaterials* **28**(15), 2465–2478 (2007).
10. D. L. Wetzel et al., "Imminent cardiac risk assessment via optical intravascular biochemical analysis," *Analyst* **134**(6), 1099–1106 (2009).
11. P. A. West et al., "Fourier transform infrared spectral analysis of degenerative cartilage: an infrared fiber optic probe and imaging study," *Appl. Spectrosc.* **58**(4), 376–381 (2004).
12. C. Krafft, "Vibrational spectroscopic imaging of soft tissue," Chap. 3 in *Infrared and Raman Spectroscopic Imaging*, R. Salzer and H. W. Seisler, Eds., pp. 113–147, WILEY-VCH Verlag GmbH & Co. KGaA, Weinheim, Germany (2009).
13. K. A. Morris et al., "Vibrational spectroscopic imaging of hard tissues," Chap. 4 in *Infrared and Raman Spectroscopic Imaging*, R. Salzer and H. W. Seisler, Eds., pp. 149–171, WILEY-VCH Verlag GmbH & Co. KGaA, Weinheim, Germany (2009).
14. H. C. Canuto et al., "Characterization of skin abnormalities in a mouse model of osteogenesis imperfecta using high resolution magnetic resonance imaging and Fourier transform infrared imaging spectroscopy," *NMR Biomed.*, **25**(1), 169–176 (2011).
15. B. C. Herman et al., "Molecular analysis of arterial remodeling: a novel application of infrared imaging," *Proc. SPIE* **7182**, 7182-H1–7182-H12 (2009).
16. K. Lui et al., "Modification of the extracellular matrix following myocardial infarction monitored by FTIR spectroscopy," *Biochim. Biophys. Acta* **1315**(2), 73–77 (1996).
17. K. Z. Liu, I. M. Dixon, and H. H. Mantsch, "Distribution of collagen deposition in cardiomyopathic hamster hearts determined by infrared microscopy," *Cardiovasc. Pathol.* **8**(1), 41–47 (1999).
18. P. S. Bromberg, K. M. Gough, and I. M. C. Dixon, "Collagen remodeling in the extracellular matrix of the cardiomyopathic Syrian hamster heart as assessed by FTIR attenuated total reflectance spectroscopy," *Can. J. Chem.* **77**(11), 1843–1855 (1999).
19. K. Gough, "Fourier transform infrared evaluation of microscopic scarring in the cardiomyopathic heart: effect of chronic AT1 suppression," *Anal. Biochem.* **316**(2), 232–242 (2003).
20. T. T. Yang et al., "Histopathology mapping of biochemical changes in myocardial infarction by Fourier transform infrared spectral imaging," *Forensic Sci. Int.* **207**(1–3), e34–e39 (2011).
21. R. C. Scott et al., "Targeting VEGF-encapsulated immunoliposomes to MI heart improves vascularity and cardiac function," *FASEB J.* **23**(10), 3361–3367 (2009).
22. R. C. Scott et al., "Targeted delivery of antibody conjugated liposomal drug carriers to rat myocardial infarction," *Biotechnology* **96**(4), 795–802 (2007).
23. B. Wang et al., "The scar neovasculature after myocardial infarction in rats," *Am. J. Physiol.: Heart Circ. Physiol.* **289**(1), H108–H113 (2005).
24. I. Adt et al., "FTIR spectroscopic discrimination of *Saccharomyces cerevisiae* and *Saccharomyces bayanus* strains," *Can. J. Microbiol.* **56**(9), 793–801 (2010).
25. C. Delcayre and B. Swynghedauw, "Molecular mechanisms of myocardial remodeling. The role of aldosterone," *J. Mol. Cell. Cardiol.* **34**(12), 1577–1584 (2002).
26. A. C. Ruifrok and D. A. Johnston, "Quantification of histochemical staining by color deconvolution," *Anal. Quant. Cytology Histology* **23**(4), 291–299, (2001).
27. J. N. Cohn, R. Ferrari, and N. Sharpe, "Cardiac remodeling—concepts and clinical implications: a consensus paper from an international forum on cardiac remodeling. Behalf of an International Forum on Cardiac Remodeling," *J. Am. Coll. Cardiol.* **35**(3), 569–582 (2000).
28. M. Jackson et al., "Beware of connective tissue proteins: assignment and implications of collagen absorptions in infrared spectra of human tissues," *Biochim. Biophys. Acta* **1270**(1), 1–6 (1995).
29. D. L. Wetzel, G. R. Post, and R. A. Lodder, "Synchrotron infrared microspectroscopic analysis of collagens I, III, and elastin on the shoulders of human thin-cap fibroatheromas," *Vib. Spectrosc.* **38**(1–2), 53–59 (2005).
30. C. Petibois et al., "Analysis of type I and IV collagens by FT-IR spectroscopy and imaging for a molecular investigation of skeletal muscle connective tissue," *Anal. Bioanal. Chem.* **386**(7–8), 1961–1966 (2006).
31. P. A. West et al., "Fourier transform infrared imaging spectroscopy analysis of collagenase-induced cartilage degradation," *J. Biomed. Opt.* **10**(1), 14015 (2005).
32. X. Bi et al., "Fourier transform infrared imaging and MR microscopy studies detect compositional and structural changes in cartilage in a rabbit model of osteoarthritis," *Anal. Bioanal. Chem.* **387**(5), 1601–1612 (2007).
33. D. C. Sheeshan and B. B. Hrapchak, *Theory and Practice of Histotechnology*, The Mosby C. V. Company, Saint Louis (1980).
34. J. Kierman, *Histological and Histochemical Methods : Theory and Practice*, 4th Ed., Scion, Bloxham, UK (2008).
35. J. Chen et al., "Assessment of cardiovascular fibrosis using novel fluorescent probes," *PloS One* **6**(4), e19097 (2011).
36. L. C. Junqueira, G. Bignolas, and R. R. Brentani, "Picrosirius staining plus polarization microscopy, a specific method for collagen detection in tissue sections," *Histochem. J.* **11**(4), 447–455 (1979).
37. L. Rich and P. Whittaker, "Collagen and picrosirius red staining: a polarized light assessment of fibrillar hue and spatial distribution," *Braz. J. Morphol. Sci.* **22**(2), 97–104 (2005).
38. M. Kitamura et al., "Collagen remodeling and cardiac dysfunction in patients with hypertrophic cardiomyopathy: the significance of type III and VI collagens," *Clin. Cardiol.* **24**(2), 325–329 (2001).
39. N. Morishita et al., "Sequential changes in laminin and type IV collagen in the infarct zone," *Jpn. Circ. J.* **60**(2), 108–114 (1996).

40. S. Wei et al., "Left and right ventricular collagen type I/III ratios and remodeling post-myocardial infarction," *J. Card. Failure* **5**(2), 117–126 (1999).
41. R. Wayne, *Light and Video Microscopy*, Academic Press/Elsevier, Amsterdam; Boston (2009).
42. S. G. Kazarian and K. L. A. Chan, "Applications of ATR-FTIR spectroscopic imaging to biomedical samples," *Biochim. Biophys. Acta* **1758**(7), 858–867 (2006).
43. F.-N. Fu, M. P. Fuller, and B. R. Singh, "Use of Fourier transform infrared/attenuated total reflectance spectroscopy for the study of surface adsorption of proteins," *Appl. Spectrosc.* **47**(1), 98–102 (1993).
44. B. R. Singh and M. P. Fuller, "FT-IR in combination with the attenuated total reflectance technique: a very sensitive method for the structural analysis of polypeptides," *Appl. Spectrosc.* **45**(6), 1017–1021 (1991).
45. K. A. Oberg and A. L. Fink, "A new attenuated total reflectance Fourier transform infrared spectroscopy method for the study of proteins in solution," *Anal. Biochem.* **256**(1), 92–106 (1998).
46. M. Carbonaro and A. Nucara, "Secondary structure of food proteins by Fourier transform spectroscopy in the mid-infrared region," *Amino Acids* **38**(3), 679–690 (2010).
47. N. P. Camacho et al., "FTIR microscopic imaging of collagen and proteoglycan in bovine cartilage," *Biopolymers* **62**(1), 1–8 (2001).
48. S. Waxman et al., "In vivo validation of a catheter-based near-infrared spectroscopy system for detection of lipid core coronary plaques: initial results of the SPECTACL study," *J. Am. Coll. Cardiol. Cardiovasc. Imaging* **2**(7), 858–868 (2009).